Technical Memorandum No. 33-178

An Electrostatically Driven Dynamic Capacitor

J. R. Locke

JET PROPULSION LABORATORY
CALIFORNIA INSTITUTE OF TECHNOLOGY
PASADENA, CALIFORNIA

July 15, 1964

Technical Memorandum No. 33-178

An Electrostatically Driven Dynamic Capacitator

J. R. Locke

Raymond L. Heacock, Chief
Space Instruments Development Section

JET PROPULSION LABORATORY
CALIFORNIA INSTITUTE OF TECHNOLOGY
PASADENA, CALIFORNIA

July 15, 1964

18 31

Prepared Under Contract No. NAS 7-100
National Aeronautics & Space Administration

CONTENTS

FIGURES

ABSTRACT

In the measurement of very small currents (i.e., 10^{-13} amp), the vibrating-capacitor electrometer can be considered a pre-eminent instrument. But, because of the prohibitive weight of most vibrating capacitors, this type of electrometer has been limited primarily to laboratory applications. This Report introduces a vibrating capacitor that weighs approximately an ounce and is roughly the size of a power transistor, which makes it ideally suited for space-flight applications. A description of the capacitor's fundamental operating principles, its function as part of an electrometer amplifier, and the history of its development to date is presented.

Although most of the major problems of the vibrating capacitor have been overcome, effort is continuing to refine further the pickup transducer, the method of mounting, and the technology related to the control of contact potential.

I. INTRODUCTION

The electrostatically driven dynamic capacitor produces a sinusoidally varying output signal proportional to a dc-input signal. This device is primarily intended to be a modulator in electrometer-amplifier applications, such as in the solar-plasma experiment flown on *Mariner 2* (Ref. 1).

Work performed at the Ames Research Center (Ref. 2) on a pressure transducer was responsible for the idea and for initiation of a study contract executed by the Kinelogic Corporation of Pasadena.[1] The prospect of developing a device to perform the same function as the dynamic capacitor flown on *Mariner 2*, but much smaller in size and lighter in weight, provided the incentive for this investigation.

The discussion that follows will present an elementary explanation of the operating principles of the device, its function as part of an electrometer circuit, significant design parameters and their relationship to the electrometer, and a brief chronology of the problems and progress to date.

[1]29 South Pasadena Avenue, Pasadena, California.

II. PRINCIPLES OF OPERATION

As an aid to the following discussion, the operational drawing of Fig. 1 will be used.

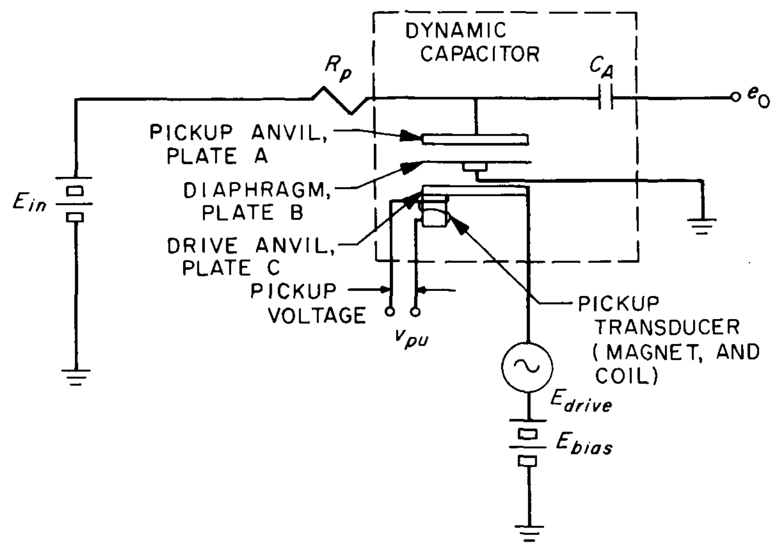

Fig. 1. Operational drawing of the dynamic capacitor

The pickup anvil, diaphragm, and drive anvil may be thought of as circular disks forming two parallel-plate capacitors. The diaphragm is mounted at its center and is capable of vibrating in a fundamental mode with a natural resonant frequency.

To understand how the device converts a dc signal into an ac signal, consider the simplified version of the pickup anvil and diaphragm shown in Fig. 2.

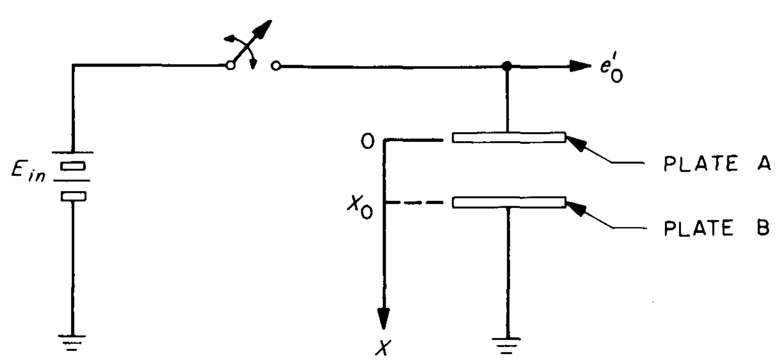

Fig. 2. Idealized version of the pickup anvil and diaphragm

Assume that the circular plate A is fixed in position and that plate B is free to move along the indicated X axis. At the time $t = 0$, with plate B at the position $X = X_0$, the switch is closed, causing a charge Q to enter the parallel-plate capacitor formed by these two plates. Then

$$Q = C_0 E_{in} \tag{1}$$

where

$$C_0 = \frac{\epsilon A}{X_0} \tag{2}$$

and A = area of plates and ϵ = dielectric constant.

With the capacitor now charged to Q, the switch is opened. Next, assume there is a means of varying the position of plate B so that its distance from plate A is given by

$$X = X_0 + D \sin \omega_0 t \tag{3}$$

where D is the maximum displacement from X_0.

Under these conditions, the output voltage would vary sinusoidally as shown in the following analysis:

$$e_0' = \frac{Q}{C} \tag{4}$$

$$C = \frac{\epsilon A}{X} = \frac{\epsilon A}{X_0 + D \sin \omega_0 t} \tag{5}$$

Substituting Relationships (1), (2) and (5) into Eq. (4), the output voltage may be expressed as

$$e_0' = E_{in} + E_{in} \frac{D}{X_0} \sin \omega_0 t \tag{6}$$

If a coupling capacitor C_A is used, as shown in Fig. 1, the output voltage is devoid of the dc term and becomes

$$e_0 = E_{in} \frac{D}{X_0} \sin \omega_0 t \tag{7}$$

Replacing the time varying expression e_0 with its corresponding rms equivalent, we may rearrange slightly and evolve an expression called the conversion efficiency

$$\eta \triangleq \frac{(e_0)_{rms}}{E_{in}} = \frac{D}{(2)^{1/2} X_0} \tag{8}$$

Although the actual device is not free to move at the center, the assumption of parallelism of the plates is a very good approximation of actual performance because the deflection of the diaphragm is very small with respect to its diameter. D then becomes the displacement averaged over the surface of the diaphragm at a time of maximum displacement.

In the idealized case of Fig. 2, a switch is used to maintain a charge on the plates that is proportional to E_{in}. Again, referring to Fig. 1, the resistor R_p effectively performs this function for the actual dynamic capacitor, where its value is chosen in such a manner that

$$R_p (C_A + C_0) >> \frac{1}{\omega_0} \tag{9}$$

where C_0 = rest capacitance associated with plates A and B, and ω_0 = vibration frequency of the diaphragm.

Besides performing the function just described, R_p limits the input current in the event that the diaphragm should clash with the pickup anvil, and it serves to isolate the device from stray capacitance at the input. To appreciate this second point more fully, consider the following alternate approach for the expression of the conversion efficiency.

$$C = \frac{Q}{v}$$

$$\frac{dc}{dv} = - \frac{Q}{v^2}$$

$$Q = vC$$

$$\frac{dC}{dv} = -\frac{C}{v}$$

rearranging

$$\frac{dv}{v} = -\frac{dC}{C}$$

approximating

$$\frac{\Delta v}{v} = -\frac{\Delta C}{C}$$

$$\frac{(\Delta v)_{max}}{(2)^{1/2} E_{in}} \triangleq \eta \tag{10}$$

therefore

$$\eta = \frac{\Delta C_{max}}{(2)^{1/2} C_0} \tag{11}$$

From Expression (11) it can be seen that the stray capacity would be added to C_0 and would decrease conversion efficiency η.

The bias voltage (Fig. 1) allows the output signal to be at the same frequency as the drive voltage, which simplifies demodulation in the electrometer circuit. An explanation of the bias-frequency relationship is most easily seen from Expression (12), which relates the force between the parallel plates of a capacitor and the applied voltage.

$$F = \frac{1}{2} \frac{\epsilon A v^2}{y^2} \tag{12}$$

Consider first the case of driving the dynamic capacitor without a bias

$$v = v_{\max} \sin \omega_D t$$

$$v^2 = v_{\max}^2 \sin^2 \omega_D t$$

$$= \frac{v_{\max}^2}{2} (1 - \cos 2\omega_D t) \tag{13}$$

For the force to be applied at the resonant frequency, $\omega_0 = 2\omega_D$ or $\omega_D = \frac{1}{2}\omega_0$, where ω_D = drive frequency and ω_0 = natural resonant frequency.

Next consider the case where a bias voltage is used

$$v = v_{\text{bias}} + v_{\max} \sin \omega_D t$$

$$v^2 = v_{\text{bias}}^2 + 2\, v_{\text{bias}}\, v_{\max} \sin \omega_D t + v_{\max}^2 \sin^2 \omega_D t$$

$$= \left(v_{\text{bias}}^2 + \frac{v_{\max}^2}{2} \right) + 2\, v_{\text{bias}}\, v_{\max} \sin \omega_D t - \frac{v_{\max}^2 \cos 2\omega_D t}{2} \tag{14}$$

If the Q_0 (Q_0 = Energy stored × 2π/Energy dissipated per cycle) of the vibrating diaphragm is high, its response to any driving impulse at a frequency other than the natural resonant frequency of the diaphragm will be greatly attenuated. Therefore, only the fundamental frequency component of Eq. (14) is effective in providing vibratory motion of the diaphragm. The dynamic capacitor can then be driven with a voltage of the same frequency as the output frequency of the dynamic capacitor.

In Eq. (12), variations in y have been neglected because the time-varying displacement is small compared with the mean separation of the plates.

Experimentally observed resonant frequencies of the dynamic capacitor have shown good correlation with results predicted by Timoshenko (Ref. 3) for a circular plate with its center fixed; namely

$$f_0 = \frac{K}{r_e^2} \left(\frac{g E T^2}{12 \rho (1 - \gamma^2)} \right)^{1/2} \tag{15}$$

where

K = mode constant of the vibration

g = gravitational constant

E = modulus of elasticity

T = diaphragm thickness

ρ = density of the material

γ = Poisson's ratio

$r_e = r_0 - r_i$ = effective diaphragm radius

r_0 = outer radius of the diaphragm

r_i = outer radius of the center support

Substituting values for the various constants, and having experimentally determined the mode constant to be approximately 0.45, Eq. (15) reduces to the convenient form of

$$f_0 = (0.45)\,(60{,}900)\,\frac{T}{r_e^2} \text{ cps} \tag{16}$$

where T and r_e are expressed in inches.

In concluding this discussion on the principles of operation, an explanation of the pickup transducer (Fig. 1,) is necessary. The function of the pickup transducer is most easily understood in terms of Fig. 3. The pickup transducer provides a feedback signal, which is independent of the input voltage to the dynamic capacitor, but proportional to the conversion efficiency. This feedback signal forces the oscillator to provide constant drive to the dynamic capacitor at its mechanical-resonant frequency. The mechanism by which the oscillator is able to track the resonant frequency of the diaphragm can be understood in terms of the Barkhausen criterion for oscillation

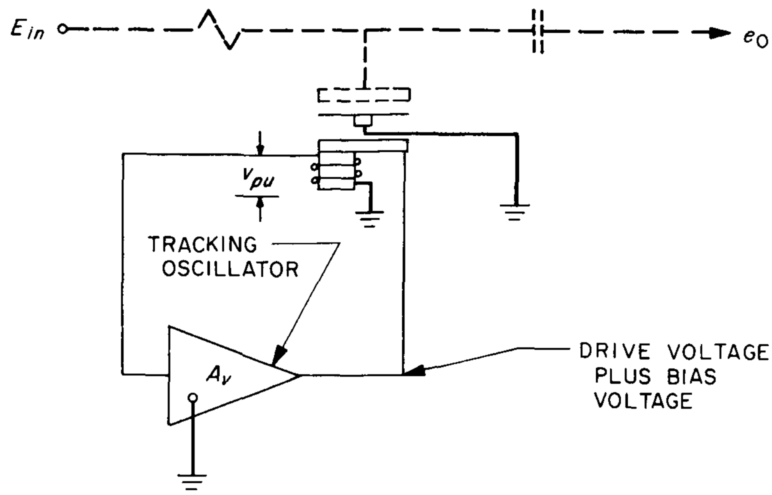

Fig. 3. Pickup transducer and tracking oscillator

$$A_v(s)\,\beta(s) = 1 \tag{17}$$

where

$$A_v(s) \triangleq \frac{e_{\text{drive}}}{v_{\text{pu}}} \quad \text{(Amplifier Gain)}$$

$$\beta(s) \triangleq \frac{v_{\text{pu}}}{e_{\text{drive}}}$$

$$s \triangleq \text{Laplace operator}$$

From the definition given for $\beta(s)$, it can be seen that its characteristics are determined by the dynamic capacitor. Because the frequency response of $\beta(s)$, is similar to that of a high Q (200 to 900) tank circuit, the oscillator closely tracks the mechanical-resonant frequency of the diaphragm. Figure 4 illustrates how the pickup voltage is generated.

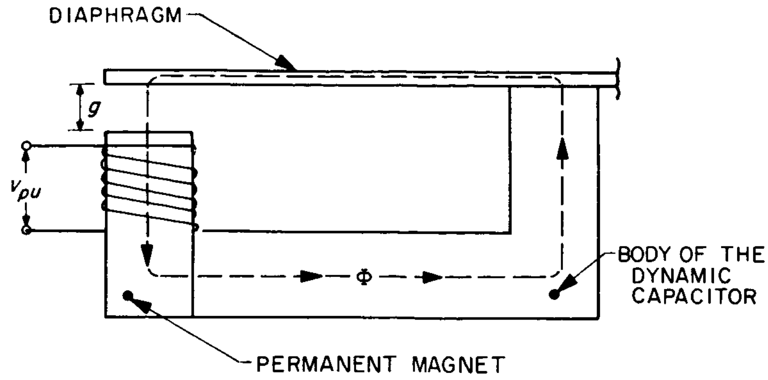

Fig. 4. Simplified version of magnetic circuit of the pickup transducer

$$\Phi = \frac{\mathcal{F}}{\mathfrak{R}_M + \mathfrak{R}_B + \mathfrak{R}_D + \mathfrak{R}_g} \tag{18}$$

where

$\mathcal{F}$ = magneto-motive force of the permanent magnet

$\mathfrak{R}_M$ = reluctance of the magnet

$\mathfrak{R}_B$ = reluctance of the body of the dynamic capacitor

$\mathfrak{R}_D$ = reluctance of the diaphragm

$\mathfrak{R}_g$ = reluctance of the air gap

Φ = magnetic flux

The reluctance of the air gap is much higher than the reluctance of other materials, since they are magnetic; thus

$$\Phi \approx \frac{\mathcal{F}}{\mathfrak{R}_g} \tag{19}$$

$$\mathfrak{R}_g = \frac{g}{\mu A_a}$$

where

g = air-gap length

μ = permeability of air

A_a = effective cross-sectional area of the air gap

$$\Phi \approx \frac{\mathcal{F}}{g} \mu A_a$$

$$v_{pu} = N \frac{d\Phi}{dt} = -N \frac{\mu A_a \mathcal{F}}{g^2} \cdot \frac{dg}{dt}$$

where

$$g = g_0 + \Delta g_{max} \cos \omega t$$

$$\frac{dg}{dt} = -\omega \Delta g_{max} \sin \omega t$$

if

$$g_0 >> \Delta g_{max}$$

Then

$$g^2 \approx g_0^2$$

$$v_{pu} \approx \frac{N\mu A_a \mathcal{F} \omega \Delta g_{max}}{g_0^2} \sin \omega t \qquad (20)$$

III. THE DYNAMIC CAPACITOR AND THE ELECTROMETER

To appreciate the design requirements for the dynamic capacitor, it is necessary to understand how they relate to the electrometer amplifier of which the dynamic capacitor is a part. The block diagram of Fig. 5 represents the typical form of the electrometer in which the dynamic capacitor is used.

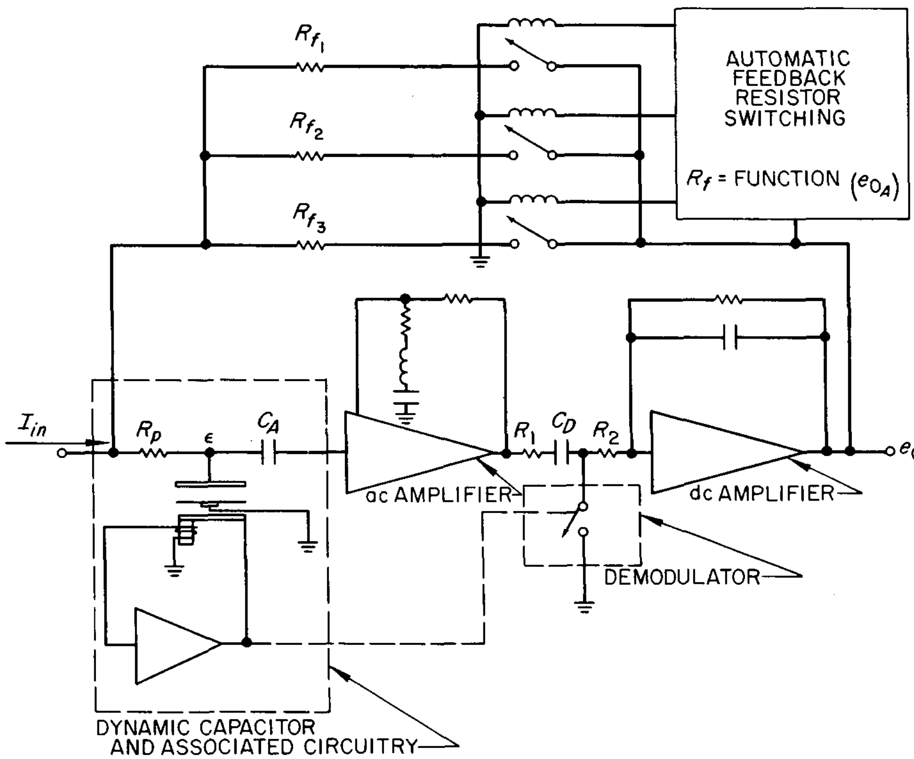

Fig. 5. Block diagram of a typical electrometer that uses a dynamic capacitor

For the initial discussion, the more simplified diagram of Fig. 6 will be helpful, where A_T = total forward gain = e_{0_A}/ϵ, and Z_{in} = input impedance (determined almost exclusively by the dynamic capacitor).

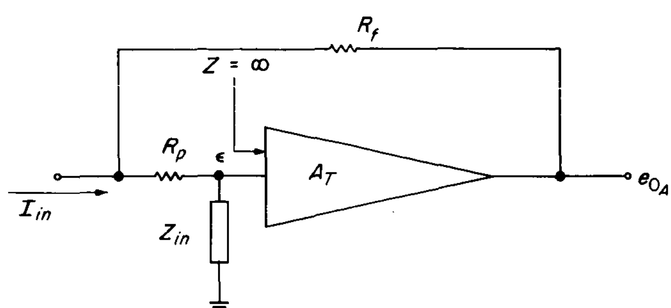

Fig. 6. Simplified version of the electrometer

To obtain the transfer function of the electrometer, superposition may be employed as follows:

$$\epsilon = \frac{Z_{in}}{Z_{in} + R_f + R_p} e_{0_A} + \frac{R_f Z_{in}}{Z_{in} + R_f + R_p} I_{in} \tag{21}$$

$$\epsilon = \frac{e_{0_A}}{A_T} \tag{22}$$

$$\beta = \frac{e_f}{e_{0_A}} = \frac{Z_{in}}{Z_{in} + R_f + R_p} \tag{23}$$

where e_f = voltage fed back from the output. Substituting (22) and (23) into (21) and solving for e_{0_A}/I_{in}, we get

$$Z_T \triangleq \frac{e_{0_A}}{I_{in}} = R_f \left[\frac{A_T \beta}{1 - A_T \beta} \right] \tag{24}$$

From Eq. (24) it can be seen that the dynamic capacitor is primarily significant as it affects the loop gain $A_T\beta$. The gain expression A_T is a function of the conversion efficiency, as indicated in Eq. (25).

$$A_T \triangleq \frac{e_{0_A}}{\epsilon} = \eta A_{ac} K_{dem} A_{dc} \tag{25}$$

where

η = conversion efficiency of the dynamic capacitor

A_{ac} = voltage gain of the ac amplifier

K_{dem} = demodulation efficiency

A_{dc} = voltage gain of the dc amplifier

The feedback ratio β is given by Eq. (23). Since the input impedance of the electrometer is determined primarily by the insulation resistance of the dynamic capacitor, the dynamic capacitor is also of major importance in determining β.

One of the design parameters that has occupied considerable attention in the development of the electrostatically driven dynamic capacitor is the stability of the conversion efficiency with time and temperature. To understand how this variation influences the operation of the electrometer, the scalar form of Eq. (24) is helpful

$$R_T = R_f \frac{F_0}{1 - F_0} \tag{26}$$

where F_0 = dc value of the loop gain $A_T \beta_0$ (−1000 is a typical value).

Differentiating R_T with respect to F_0 we get

$$\frac{dR_T}{dF_0} = \frac{R_f}{(1 - F_0)^2} \tag{27}$$

Rearranging Eq. (27) and dividing by Eq. (26) yields

$$\frac{dR_T}{R_T} = \frac{dF_0}{F_0} \cdot \frac{1}{(1 - F_0)} \tag{28}$$

For small incremental changes, the following approximation is valid:

$$\frac{\Delta R_T}{R_T} \approx \frac{\Delta F_0}{F_0} \cdot \frac{1}{(1 - F_0)}$$

Using Eq. (25), and considering everything but the conversion efficiency η as a constant, the effect of temperature variations on the closed-loop performance can be evaluated. Specifications on the conversion efficiency allow a change of ±10% from the room temperature value over the temperature range of −20 to +90°C. Substituting these values into Eq. (29) gives the following results:

$$\frac{\Delta R_T}{R_T} = \frac{(-1100 + 900)}{-1000} \cdot \frac{1}{1 + 1000} \approx 0.02\% \tag{29}$$

From the example, it can be seen that if the capacitor is operating within specifications, it causes no serious problem.

Variations in the resonant frequency can be a more severe problem, because both the gain of the ac amplifier A_{ac} and the demodulation efficiency K_{dem} are affected.

Referring to Fig. 5, it will be observed that the ac amplifier utilizes a series-tuned circuit in the feedback loop to eliminate intermodulation distortion, reduce noise, and control the bandwidth. The closed-loop frequency response of the ac amplifier is characterized by the frequency response of this tuned circuit and, therefore, is sharply selective around the room-temperature resonant frequency of the dynamic capacitor. If the frequency of the dynamic capacitor changes substantially, operation of the ac amplifier is translated down the skirts of the response curve with a resulting decrease in gain. Also, by detuning the ac amplifier, a phase shift occurs that directly affects the demodulation efficiency, as can be seen in Eq. (30)

$$K_{dem} = \frac{2(2)^{1/2}}{\pi} \frac{R_2}{2R_1 + R_2} \cos\theta \tag{30}$$

where θ = phase angle between the voltage driving the demodulator and the ac-amplifier output voltage. R_1 and R_2 are shown in Fig. 5.

Another problem associated with the operation of the dynamic capacitor is what might be called contact-potential variations. In behavior, its characteristics are those of a potential caused by dissimilarity of metals. But, in light of the precautions that have been taken to minimize any such dissimilarities, and the relatively large potentials that have been measured, it seems likely that the more commonly used meaning of contact potential isn't accurate. In effect, it appears as a battery interposed between plate B and ground (Fig. 7). As a functional aid to the understanding of what it is, the measuring method will be described. Figure 7 illustrates the actual test setup used. Referring to Eq. (8)

$$\eta = \frac{(e_0)_{rms}}{E_{in}} \tag{8}$$

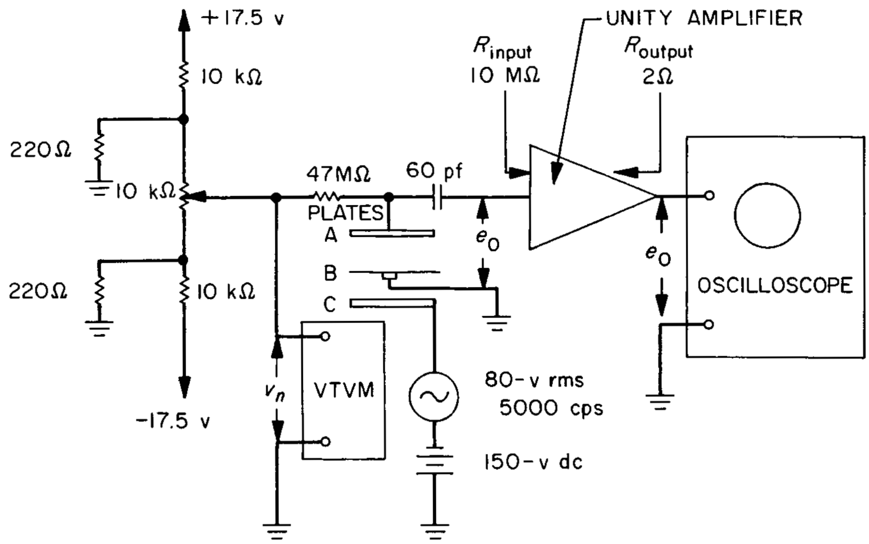

Fig. 7. Test setup used for measuring contact potential

and substituting

$$E_{in} = v_c - v_n$$

where

v_c = contact potential

v_n = null voltage

then

$$(e_0)_{rms} = \eta (v_c - v_n) \tag{31}$$

By adjusting the null voltage so that it is equal to the contact potential, the output voltage goes to zero. A measurement of the null voltage producing zero output voltage is therefore a measurement of the contact potential.

To analyze the effect of the contact potential on the operation of the electrometer, the block diagram shown in Fig. 8 will be used.

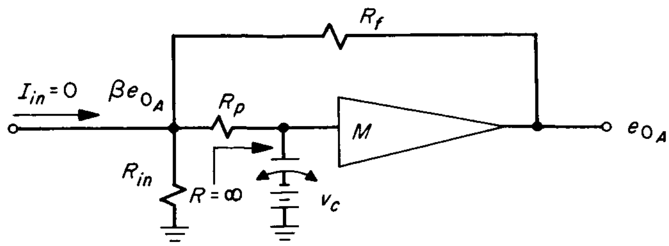

Fig. 8. Electrometer and virtual contact-potential battery

$R_{in} \triangleq$ input resistance

$$M \triangleq \frac{A_T}{\eta} \tag{32}$$

$$\beta_0 \triangleq \frac{R_{in}}{R_{in} + R_f} \tag{33}$$

With the aid of Fig. 8 and Eq. (32) and (33), an expression can be written for the output voltage as a function of the contact potential

$$\eta(\beta_0 e_{0_A} - v_c)M = e_{0_A}$$

Rearranging and solving for e_{0_A}

$$e_{0_A} = -\frac{v_c \eta M}{1 - \eta M \beta_0}$$

$$= -\frac{v_c A_T}{1 - A_T \beta_0}$$

$$= \frac{-v_c}{\beta_0}\left[\frac{A_T \beta_0}{1 - A_T \beta_0}\right]$$

if

$$|A_T \beta_0| >> 1$$

(which it is), then

$$e_{0_A} \approx + \frac{v_c}{\beta_0} \tag{34}$$

From Eq. (34), two important pieces of information can be seen. First and most important, the contact potential, and any drifts associated with it, are seen directly at the output, unlike the other parameters that affected only the loop gain. Second, the contact potential is seen at the output, multiplied by the reciprocal of the feedback ratio β. Since the feedback ratio is highly dependent on the input resistance (as can be seen in Eq. (33), and the input resistance is essentially that of the dynamic capacitor, the need for the dynamic capacitor to have high insulation resistance becomes apparent.

IV. CHRONOLOGY OF THE PROBLEMS AND PROGRESS

The results of the study performed by the Kinelogic Corporation prompted the awarding of a supporting research and technology contract to them for the design, development, and fabrication of 10 dynamic capacitors. This number was later increased to 13 when further development was found to be necessary.

Specifications for the device were based, in part, on the performance of the dynamic capacitor flown on *Mariner 2*, with the additional constraints of a lighter weight and a higher mechanical-resonant frequency. The major specifications are listed in Table 1.

Table 1. Primary specifications for dynamic capacitor

Parameter	Specification
Conversion efficiency η	7% minimum
Allowable variation of η over the temperature range of −20 to +90°C	± 10% of room temperature value
Resonant frequency (f_0)	3000 cps minimum
Allowable variation of f_0 over the temperature range of −20 to +90°C	± 0.2% of room temperature value
Contact potential (v_c)	
Maximum v_c	$\lvert \pm 50 \rvert$ mv
Maximum $\frac{dv_c}{dt}$ (temperature)	$\lvert \pm 100 \rvert \mu v/°C$
Insulation resistance at input with all other terminals grounded	$10^{13} \Omega$ minimum
Maximum weight	1.8 oz

The first dynamic capacitor developed by Kinelogic Corporation used a thin diaphragm (0.2 mil), which was maintained under high tension. The thinness made assembly difficult and the diaphragm subject to damage. To operate at the desired frequency, it was necessary to place the diaphragm under high tension, which proved to be difficult because of the threat of exceeding the elastic limit of the materials. To overcome the problems encountered, the thickness of the diaphragm was increased to 3 mils, but, by using the thicker diaphragm, Kinelogic was unable to get frequencies high enough to meet the Jet Propulsion Laboratory specifications.

Because of the above difficulties, a disk 15-mils thick was sandwiched between the two parts of the housing without applying any tension. By using this new approach, most of the earlier problems were overcome. No longer was there a problem of getting a precise amount of tension on the diaphragm, since the disk merely was supported between the drive and pickup anvils. By going to a thicker diaphragm, the parameters governing the mechanical-resonant frequency changed, and frequencies in excess of 5 kc were obtainable.

Further testing of the capacitor revealed the following problems. Epoxy sealant had melted, causing the failure of two units. The resonant frequency and conversion efficiency were erratic when the device was subjected to temperature variations. Contact potential was measured for the first time and found to be excessive and unstable.

The first remedial step taken was to bond mechanically the diaphragm and the housing in order to prevent further failures. The various screws, parts of the anvils, the housing, spacers, and washers were made of materials that would have coefficients of expansion well-matched to minimize adverse thermal stresses, a cause of instability. A design was conceived that would do away with the large sapphire disk on which the high impedance terminals were mounted. This would allow the vacuum seal to be accomplished by using heliarc welding, thereby eliminating the need for an epoxy seal of any kind. The transducer pickup coil was relocated so that outgassing of any of its organic parts wouldn't communicate with the evacuated region and possibly contribute to the contact potential. The diaphragm and anvils were gold-plated in an attempt to minimize the contact potential, and the work area for the dynamic-capacitor project was relocated in a more isolated area so that the threat of contamination during assembly could be more effectively controlled.

In spite of the measures taken to match the thermal coefficients of expansion, excessive instability of conversion efficiency and resonant frequency were still in evidence, although slightly reduced. After considerable analysis and experimentation, it was determined that slight temperature variations were sufficient to produce large stresses in the diaphragm, which resulted from its rigid attachment to the housing.

To remedy this problem, the method of supporting the diaphragm was changed from clamping it along the edge to fixing it at the center. This solution has been enormously successful in attaining a stable resonant frequency. By using the center-support technique, the parameters determining the mechanical-resonant frequency again changed. This change resulted in a need to reduce the diameter of the diaphragm. Combining the change in diameter with certain other intrinsic properties of the design, it was possible to realize a substantial decrease in dimension and weight.

Although the conversion efficiency was made more stable by going to center-support configuration, the decreased mass of the dynamic capacitor made mounting the device considerably more critical. If improperly mounted, the terminal leads would now act as parasitic resonant systems and would rob energy from the capacitor.

Initial attempts to suppress the contact potential by gold-plating the diaphragm and anvil were unsuccessful because of a contaminated bath. To avoid this problem, the parts were next coated with gold using a vacuum deposition technique, which proved unsatisfactory because of flaking. However, the plating process was found to be adequate if supplemented with additional measures. Most important, as earlier indicated, was to ensure a plating bath free of foreign substances. Upon completion of the plating, the diaphragm and anvils must be cleansed in a basic solution to assure acid neutralization. The parts are then boiled for a prolonged period in de-ionized water. After the capacitor has been assembled, the device is prepared for evacuation by placing it at an elevated temperature and flushing it first with argon gas and then with hydrogen gas, which are used to accelerate the outgassing of gases diffused on the surfaces of metals in communication with the evacuated cavity. These techniques have resulted in a contact potential versus temperature that is well within specifications.

When the original design, using the sapphire disk, was changed to avoid the use of epoxy as a sealant, it was necessary to replace the high-impedance terminals. The types chosen were Bendix's TH 10 and TH 17 high-alumina ceramic feed-through terminals. Subsequent units built with the new terminals had a higher incidence of leakage problems. The trouble was traced to these terminals losing seal because of their inability to withstand the harsh conditions placed upon the dynamic capacitor in minimizing contact potential. Another contributing factor was the vibration of the dynamic capacitor itself.

To solve the insulator leakage problem, Kinelogic engaged the services of the Physical Sciences Corporation.[2] This organization had developed a technique which would permit pouring the molten dielectric

[2] 314 Live Oak, Arcadia, California

(Durock D117) directly around the terminals while they are held in the appropriate positions in the dynamic-capacitor housing. This method has a number of advantages, the chief one being that the leakage rate is guaranteed to be less than or equal to 10^{-14} cm^3/sec-atm. The reliability of this terminal is much higher than the Bendix terminal because of the bond between the insulator and the pin. The Bendix terminal is bonded only at the points where the pin pierces the surfaces of the insulator. The technique used by the Physical Sciences Corporation allows the metal of the pin to partially diffuse into the insulator and thereby bond the pin to the insulator along its entire length. Because the quenching process quickly drops the temperature of the dielectric from 800 to −300°F, the terminal structure is preconditioned to withstand large thermal stresses. Durock (D117) is a silico-ceramic insulation material having a resistivity of 2×10^{18} ohm-cm. Another favorable feature of the Durock terminals is that comparative tests have shown them to generate smaller strain currents than the Bendix terminals.

In changing from the edge-clamped design to the center-support configuration, the pickup transducer has experienced a substantial decrease in its ability to generate a voltage signal. Earlier edge-clamped units developed typical voltages of 60-80 mv rms. Present center-support units produce voltages in the range of 10-20 mv rms, making the job of the tracking oscillator more difficult. The air gap for the edge-clamped units was at the center of the diaphragm, the point of maximum variation. For the center-support units, the air gap closes the magnetic circuit at the perimeter of the diaphragm, as suggested in Fig. 4. Two factors have contributed to decrease the pickup voltage. The first is a decreased permeability in the diaphragm, resulting from the heat-treating process used to optimize the capacitor's resonant frequency and conversion-efficiency characteristics versus temperature. The second factor is the new magnetic circuit, which has a greater number of leakage paths. Presently a step-up transformer provides adequate signal to the oscillator.

As a final remark on the progress to date, it should be noted that insulation resistance was improved in going from the original sapphire disk to feed-through terminals. The primary improvement was attributed mainly to a smaller susceptibility to contamination and resulting surface leakage paths. Present input resistance of the device is greater than 10^{14} ohms.

Figure 9 illustrates the evolution of the capacitor from the unit flown on *Mariner 2* at the extreme left, through the intermediate edge-supported unit in the middle, to the present device shown at the far right. Figures 10 and 11 show the present unit in greater detail.

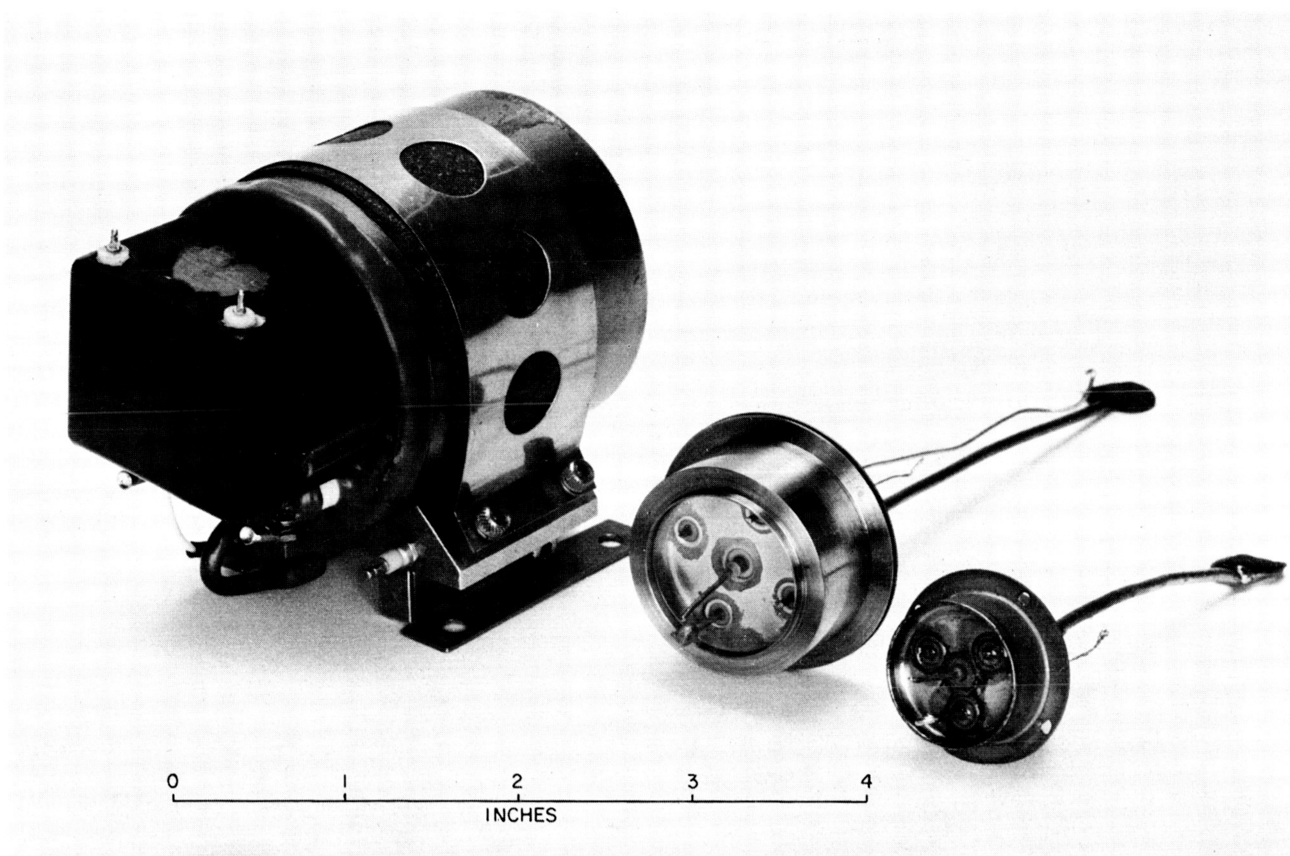

Fig. 9. *Mariner R* dynamic capacitor, edge-supported dynamic capacitor, and center-supported dynamic capacitor

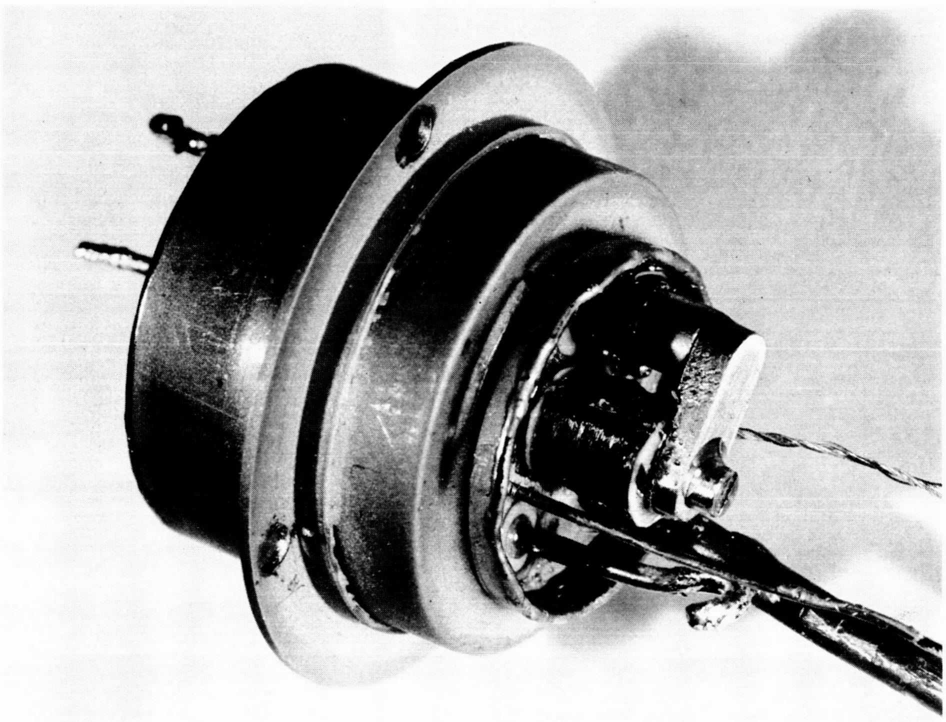

Fig. 10. View of center-supported dynamic capacitor showing drive terminals and pickup transducer

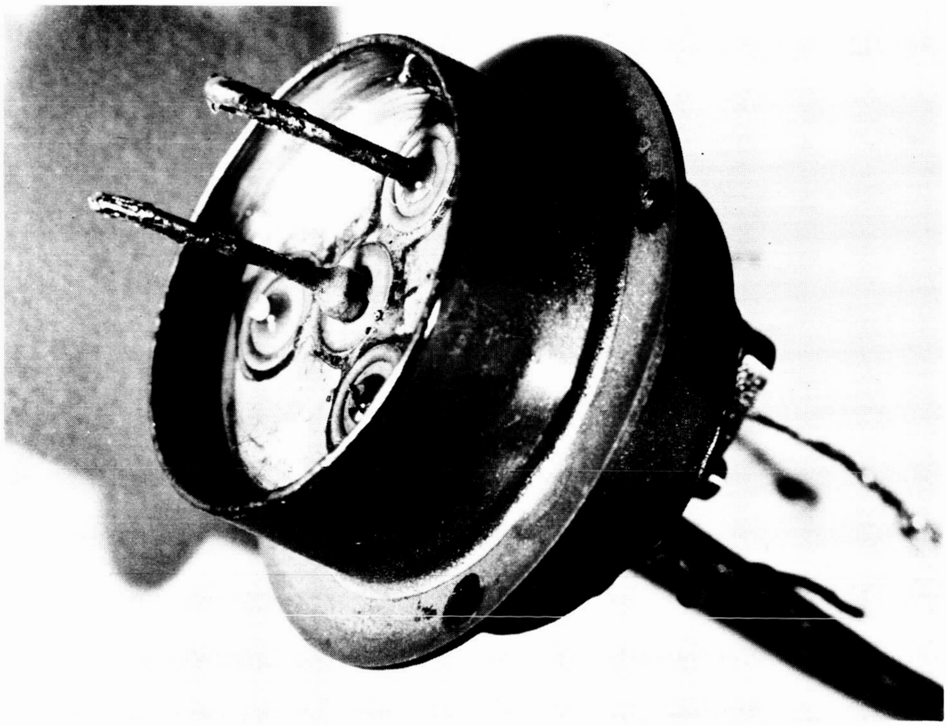

Fig. 11. View of center-supported dynamic capacitor showing input and output terminals

NOMENCLATURE

A area of plates A, B, or C

A_a effective cross-sectional area of the air gap in the magnetic circuit

A_v amplifier gain

A_T total forward gain of the electrometer amplifier

A_{ac} voltage gain of the ac amplifier

A_{dc} voltage gain of the dc amplifier

C capacitance

C_A coupling capacitor of the dynamic capacitor

C_0 quiescent capacitance between plates A and B

D amplitude of the diaphragm

E modulus of elasticity

E_{in} dc-input voltage to the dynamic capacitor

e_f portion of output voltage fed back

e_{0_A} output voltage of the electrometer amplifier

e_0 ac portion of the output voltage of the dynamic capacitor

e_0' total output voltage of the dynamic capacitor

F electrostatic force

$\mathcal{F}$ magneto-motive force

F_0 dc value of the loop gain of the electrometer amplifier

f_0 mechanical-resonant frequency

g gravitational constant

g air-gap length

g_0 quiescent air-gap length

I_{in} electrometer-amplifier input current

NOMENCLATURE (Cont'd)

K mode constant of vibration

K_{dem} demodulator efficiency

M A_T/η, voltage gain between the input of the ac amplifier and the output of the dc amplifier

N number of turns on the pickup coil

Q charge

Q_0 mechanical-resonant quality, $\left(\dfrac{2\pi \text{ energy stored}}{\text{energy dissipated per cycle}}\right)$

r_e effective diaphragm radius

r_i radius of the center support

r_0 outer radius of the diaphragm

R_f feed-back resistor

R_p input resistor of the dynamic capacitor

R_{in} input resistance to the electrometer amplifier

R_T transfer resistance

$\mathfrak{R}_B$ reluctance of the body of the dynamic capacitor

$\mathfrak{R}_D$ reluctance of the diaphragm

$\mathfrak{R}_g$ reluctance of the air gap

$\mathfrak{R}_M$ reluctance of the permanent magnet

s Laplace operator

T thickness of the diaphragm

t time

v voltage

v_c contact-potential voltage

v_n null voltage

NOMENCLATURE (Cont'd)

v_{pu}	pickup voltage
v_{bias}	bias voltage
X	distance of plate B from A
y	distance of plate B from C
X_0	quiescent distance of plate B from A
Z_T	transfer impedance
Z_{in}	input impedance to the electrometer amplifier
β	feed-back ratio
β_0	dc feed-back ratio
γ	Poisson's ratio
Δ	incremental change
ϵ	dielectric constant
ϵ	summing-point voltage
η	conversion efficiency
θ	phase angle between the voltage driving the demodulator and the ac-output voltage
μ	permeability of air
π	3.14...
ρ	density
Φ	magnetic flux
ω	angular frequency
ω_D	angular frequency of the drive voltage
ω_0	angular mechanical-resonant frequency

REFERENCES

1. Josias, Conrad, and Lawrence, James Jr., *An Instrument for the Measurement of Interplanetary Solar Plasma,* Technical Report No. 32-492, Jet Propulsion Laboratory, May 1, 1964.

2. Dimeff, J., Lane, J., and Coon, G., "New Wide Range Pressure Transducer," *The Review of Scientific Instruments,* August, 1962, pp. 804-811.

3. Timoshenko, S., *Vibration Problems in Engineering,* D. Van Nostrand Co., Inc., 1937, pp. 418-421.